Estimating Human Tactile Resolution Limits for Stimulator Design

Eden Tan

Abstract

To build a better stimulator display for the human tactile system, it is necessary to quantify the performance of that system. A fundamental component of a tactile stimulator system is an elastic layer which functions as an anti-aliasing filter. Psychophysical experiments performed measure the ability to statically perceive gratings through an intervening layer of elastic material. Spatial threshold levels are established for the subjects, and a modulation index is determined for those levels based on predicted sub-surface strain using a half-plane elastic model. Hysteresis effects observed during the tests are believed to reduce discrimination.

1 Introduction

It is known that the human finger can perceive high resolution features when placed in direct contact with an object. Points, edges, and gaps of very small size are easily discernible, as well as various patterns and shapes. A variety of experiments have been performed quantifying the limitations of the finger in distinguishing such shapes and points, among them Phillips and Johnson (1981a), Phillips and Johnson (1981c), LaMotte and Srinivasan (1987), and Phillips et al. (1992). However, these experiments have always dealt with the results of direct skin-to-surface contact, and there have been few, if any, which deal with the loss of information that comes about when the finger attempts to perceive objects through a layer of material, such as a glove.

The different types of tactile stimulators currently under investigation, such as Cohn et al. (1992), Kontarinis and Howe (1993), and Hasser and Weisenberger (1993), are

all designed to stimulate the mechanoreceptors (nerve endings) in the finger which are responsible for most of the static perception of shape. These are the Merkel cell neurite complexes, commonly referred to as SA or SA I units, and they are normally found at a depth of approximately 0.7 mm to 1.0 mm below the skin surface. This is based on the modelled depths and the actual depths of the SA I units for the macaque monkeys studied in Phillips and Johnson (1981c). Although the actual receptor depth in human fingers is unknown, this is a reasonable estimate.

To stimulate these mechanoreceptors, tactile systems generally use small pin or piston arrays which are placed against the finger and indented into the skin surface. The purpose of these indentions is to produce approximations to actual contours or surface stresses, such that the finger sensations received from them are not distinguishable from an actual contact. This is based on the idea of sampling, where given a high enough sampling density (at least four times the spatial density of the mechanoreceptors in the skin), it is possible to replicate the original signal; in this case, a contour or shape. Unfortunately, due to the high sensitivity of the human finger, the individual elements of typical stimulator arrays are sometimes detectable by the human tactile system, and thus, smooth, continuous sensations are not perceived for approximations to continuous surfaces. This occurs because of the high frequency of the SA I mechanoreceptors in the skin, which Vallbo and Johansson (1979) found to be 70 sensors/cm^2. This requires that the pins/pistons be spaced, at most, 1.2 mm apart. Cohn et al. (1992) have one of the most densely packed arrays, with 2.0 mm spacings between piston centers. Since the pistons are not sufficiently close, aliasing occurs, and the individual pistons of the stimulator array are felt. Thus, in order to produce the sensation of a continuous surface, either the pins/pistons must be moved closer to provide a higher sampling density for the mechanoreceptors, or they must be spatially low-pass filtered by some intervening layer of material to eliminate the aliasing effects.

Since manufacturing the pins/pistons closer together is difficult for such a small array, it is necessary to place some form of layer in between the finger and stimulator. By spatially low-pass filtering the data from the pins/pistons, the components of the tactile arrays may be spaced at wider intervals, which makes construction of the stimulator system easier. Using an elastic layer such as silicone rubber adequately suits this purpose, since it acts as a good anti-aliasing spatial low-pass filter. In order to produce negligible aliasing, the thickness of the layer should be twice the tactile array spacing, as found in Fearing and Hollerbach (1985). However, for current tactile stimulators, this requirement produces an extremely thick layer which reduces the amount of information received by the finger. In order to perceive high resolution shapes and contours, it is necessary to have good sensitivity (signal-to-noise ratio), which is not provided by such a thick layer. Therefore, a compromise is reached between anti-aliasing and high sensitivity by choosing a rubber thickness equal to the pin/piston spacing, as was done in Fearing (1990). The purpose of this project is to determine how well people can perceive spatial detail from a tactile display when the contact data is filtered with this intervening layer; in our case, a 2.0 mm layer of silicone rubber. This 2.0 mm thickness is chosen in order to produce a spatial low-pass filter for the 2.0 mm period density of the stimulator array used by Cohn et al. (1992). Figure 1 shows the array and finger geometry used in their tactile stimulator.

If the sub-surface strain resulting from contact with a filtered surface is known, the amplitude resolution characteristics of human fingers can be better determined. To do this, the stress/strain characteristics of the human finger are first approximated by using half-plane elastic analysis. Then, the grating patterns used in the psychophysical tests are decomposed into a series of equivalent line loads. These line loads are used to calculate the estimated strain profile perceived through the rubber layer by the SA I mechanoreceptors underneath the skin surface. Using this profile and the data derived from the psychophysical tests, a general detectable modulation factor for the average person can be

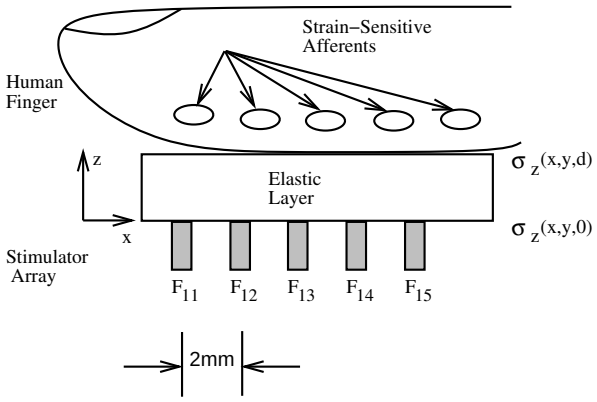

FIGURE 1. *Tactile stimulator array from Cohn, Lam, and Fearing (1992)*

calculated. The modulation factor is defined as the amplitude of the strain response of the grating pattern normalized by the DC bias associated with a smooth surface. This can be written as

$$strain \sim (1 + \mu \cos(\frac{2\pi}{period} x)) \quad (1)$$

where μ is the modulation index. If the modulation factor from a patterned surface is larger than the background noise levels of the human tactile system, a person will be able to detect the pattern underneath the rubber layer. This is similar to Weber's Law, which states that the perceptibly distinguishable levels of a system are constant proportions of the inputs (Goldstein 1980). Therefore, the modulation index can be used to predict what can be perceived by the human tactile system.

Although there are several factors and uncertainties which are not taken into account by the models used, this still allows us to better specify tactile stimulator density and force resolution necessary for perception through various materials. Thus, it will be possible to build better tactile stimulators which provide only the minimal amount of information necessary to allow the finger to perceive actual shapes and contours.

2 Model of the Human Finger

2.1 Elastic Half-Plane Method

The human finger has been previously modelled using half-plane elastic analysis (Phillips and Johnson 1981c). Although a more complex analysis could be performed, the unmodelled structure of the finger and the physical differences between people's fingers would have made such calculations useless. Also, the effects of the tissue being compressed against the bone structure is unknown. However, Fearing (1990) did a comparison between an elastic half-plane and an elastic layer with a rigid foundation. In it, he finds that there is little difference between this approximation and the simpler half-plane analysis. Thus, the elastic half-plane model is used here.

As in Phillips and Johnson (1981c), plane stress is used when modelling the finger, since the plane stress assumption agrees better with the response of the mechanoreceptors in the macaque monkey finger for their geometry. Figure 2 defines the coordinate system used in our tests and shows the orientation of the gratings, which are equivalent to the gratings and orientations used by Phillips and Johnson. In the figure, the stresses due to contact with the grating patterns are modelled as line loads, which are constant along the

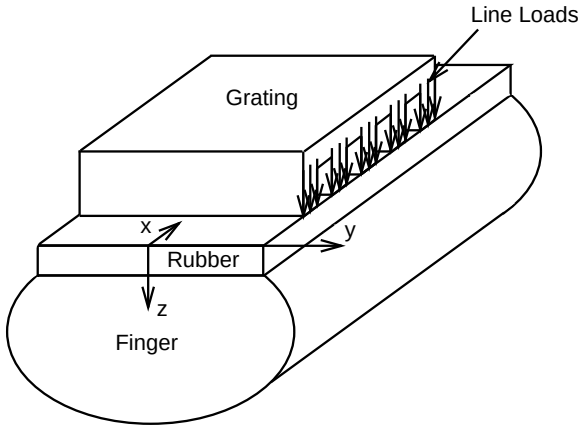

FIGURE 2. *Finger and grating geometry for plane stress assumption*

y-axis but which vary along the x-axis of the finger. A thin slice is taken from the x-z plane and is considered for planar stress analysis.

From the plane stress assumption, the stress σ_y is equal to 0 for a line load *P*. From Timoshenko and Goodier (1970), this gives the stresses and strains normal to the surfaces as

$$\sigma_x = \frac{-2Px^2z}{\pi r^4} \tag{2}$$

$$\sigma_z = \frac{-2Pz^3}{\pi r^4} \tag{3}$$

$$\tau_{xz} = \frac{-2Pxz^2}{\pi r^4} \tag{4}$$

Using these relations between stresses and strains, the normal component of strain is

$$\varepsilon_z = \frac{-2Pz}{E\pi r^4}(z^2 - \nu x^2) \tag{5}$$

where *P* (Nm^{-1}) is the force per unit length, $r^2 = x^2 + z^2$, ν is Poisson's ratio (assumed as 0.5 for an incompressible material such as rubber), and *E* is Young's modulus, which for our silicone rubber is $4x10^5$ Nm^{-2}. Calculation of the normal strain for a line load results in the equation

$$\varepsilon_z(d_o, x) = \frac{2Pd_o}{E\pi r^4}(d_o^2 - \frac{1}{2}x^2) \tag{6}$$

where d_o is the depth of the mechanoreceptors (2.7 mm: 2.0 mm from the rubber layer and 0.7 mm from the depth of the mechanoreceptors in the skin) and *r* is the distance from the line load origin ($r^2 = x^2 + {d_o}^2$).

In Phillips and Johnson (1981c), it was found that the maximum compressive strain regardless of orientation (ε_c) was the only strain response that closely approximated the SA I mechanoreceptive profiles. Thus, this strain value is also looked at. The maximum compressive strain is calculated as

$$\varepsilon_c = \frac{1}{2E}\left(\left(\frac{\sigma_x + \sigma_z}{2}\right) + 3\tau_{max}\right) \tag{7}$$

where

$$\tau_{max} = \left(\left(\frac{\sigma_z - \sigma_x}{2}\right)^2 + \tau_{xz}^2\right)^{0.5} \tag{8}$$

Calculation of the maximum compressive strain regardless of the orientation for the line load yields

$$\varepsilon_c(d_o, x) = \frac{2Pd_o}{E\pi r^4}(d_o^2 + x^2) \tag{9}$$

Here, d_o and r are the same as for the normal strain. Figure 3 shows both the normal and maximum compressive strain for the silicone rubber medium in response to a line load.

By taking the Fourier transform of the normal strain, the transfer function

$$H_n(s) = \frac{1}{E}(1 - \nu + (1 + \nu)\, 2\pi d_o|s|)\, e^{-2\pi d_o|s|} \tag{10}$$

$$= \frac{1}{E}\left(\frac{1}{2} + 3\pi d_o|s|\right) e^{-2\pi d_o|s|}$$

is produced, where s is the spatial frequency (cycles/mm). The Fourier transform of the maximum compressive strain is

$$H_c(s) = \frac{2}{E} e^{-2\pi d_o|s|} \tag{11}$$

The two transforms are shown in figure 4 and correspond to the spatial frequency response of the elastic rubber medium at a depth of 2.7 mm. As can be seen, the maximum compressive strain has a lower spatial frequency response than the normal strain.

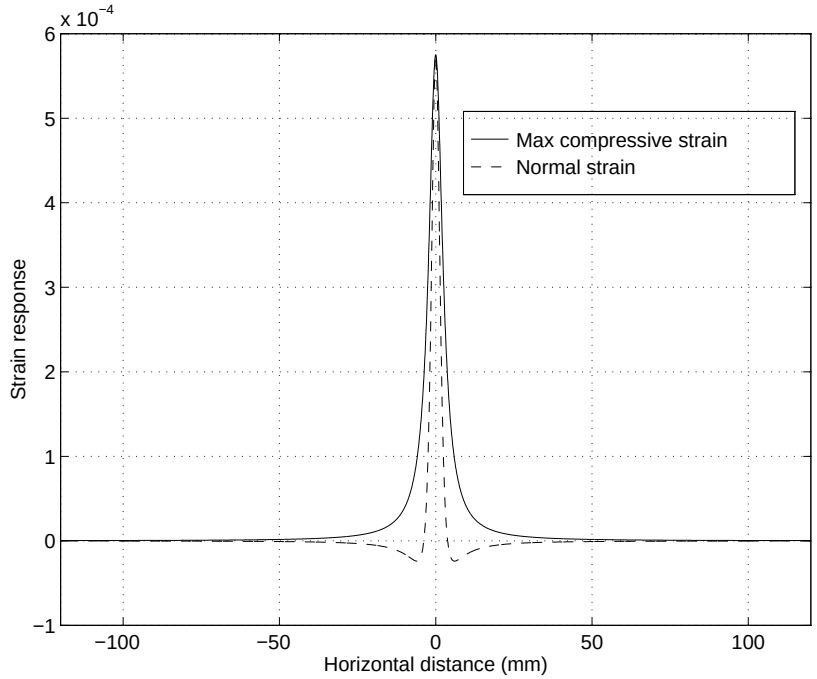

FIGURE 3. *Strain response at a depth = 2.7 mm*

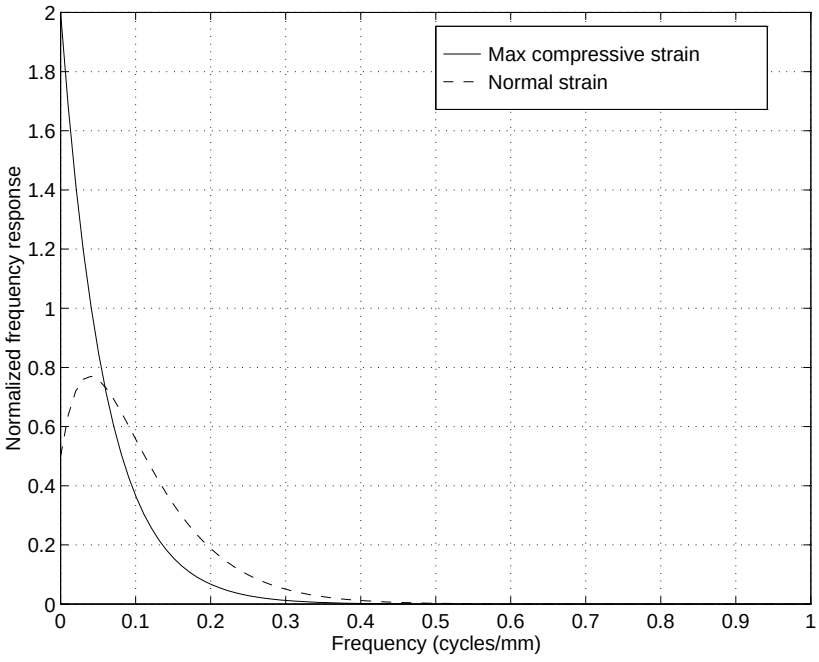

FIGURE 4. *Normalized spatial frequency response at a depth = 2.7 mm*

2.2 Strain Profile Based on Displacement/Line Load Profiles

In order to calculate a modulation factor from a given grating pattern, it is first necessary to determine what strain profiles are presented to the mechanoreceptors in the fingertip by that grating pattern. To do this, the surface deflection of the grating pattern is decomposed into a series of equivalent normal line loads, as was done in Phillips and Johnson (1981c). Then, these line loads are used to calculate the sub-surface strain profile.

The basis for calculating the set of equivalent line loads is the normal surface deflection produced by a single line load, which, from Phillips and Johnson (1981c), is

$$\begin{aligned} c(x) &= \frac{2}{\pi E}\log\frac{x_b}{x_o} && |x| < x_o \\ &= \frac{2}{\pi E}\log\frac{x_b}{|x|} && x_o < |x| < x_b \\ &= 0 && x_b < |x| \end{aligned} \tag{12}$$

This is shown in figure 5. As can be seen from equation (12), the line load has a constant deflection over its application width, which was chosen to be 50 μm. Thus, the close boundary x_o, within which the deflection is constant, has a value of 25 μm. Also, the deflection logarithmically decays outside of the impulse region. From Phillips and Johnson (1981b), it is known that the interaction of a line load on its neighboring loads is negligible at a distance greater than 3.0 mm. This was chosen as the distant boundary value x_b, which is the distance beyond which there is no surface deflection.

It is assumed in Phillips and Johnson (1981c) that the deflection is proportional to the line load magnitude. It is also assumed that the deflection function is spatially invariant, and that the overall deflection is the superposition of the deflection patterns from the individual line loads. Thus, the surface deflection $d(x)$ at a specific location x is given as

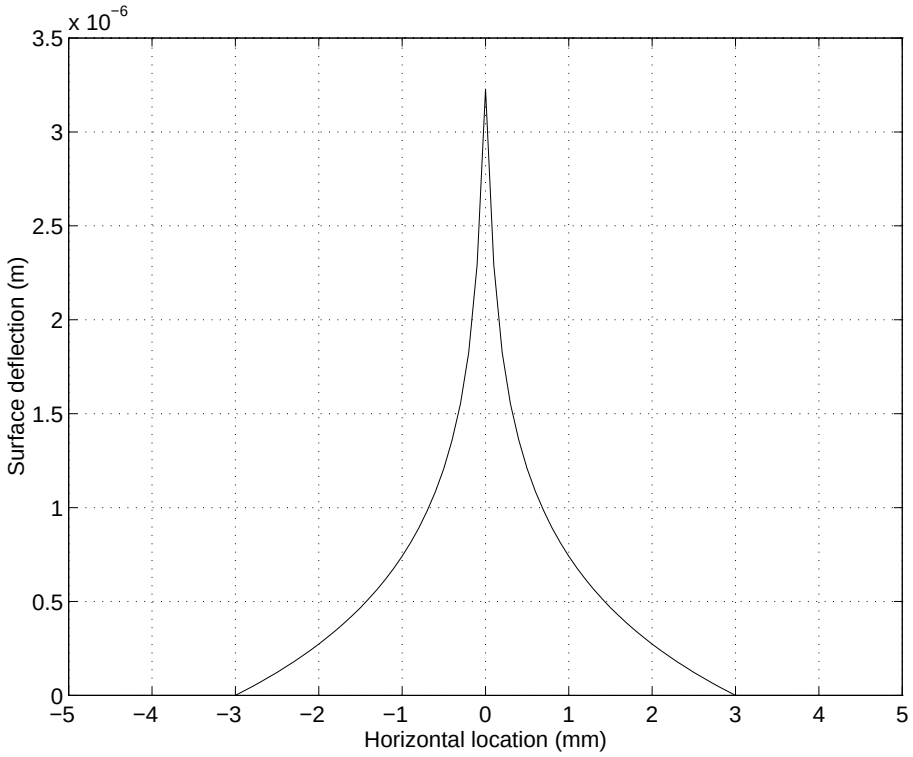

FIGURE 5. *Impulse surface deflection from a line load with* x_o *= 25* μ*m and* x_b *= 3.0 mm*

$$d(x) = \sum_{j=1}^{n} c(x - x_j)\, p(x_j) \tag{13}$$

This is the convolution sum of the deflections of the n line loads at locations x_j with pressure $p(x_j)$. If the line loads are within 3.0 mm of the deflection location x, they contribute to the deflection; if not, they do not affect it. The line load boundary condition for our case is $p = 0$. Thus, the line loads corresponding to the gaps in between the gratings are not specified as part of x_j. The line loads are spaced at 100 μm to simplify construction of the pressure profiles for grating period differences of 0.2 mm.

To calculate the surface deflection over the entire grating pattern, it is necessary to specify the locations x_i, which are the surface deflections examined. For m such locations, this results in the surface deflection equation

$$d(x_i) = \sum_{j=1}^{n} c(x_i - x_j)\, p(x_j) \tag{14}$$

from Phillips and Johnson (1981c). The surface deflection boundary condition used in our case is $d = 0$. As with p, the deflections corresponding to the gaps in between the gratings are not specified as part of x_i. Thus, both the pressure and deflection boundary conditions are equivalent. The spacings of the deflection locations examined is also chosen as 100 μm. Since the spacings and boundary conditions are the same, $x_i = x_j$ for our case. Therefore, m and n, the sizes of the deflection location vector and the line load vector, respectively, are equivalent. The value m is arbitrarily chosen as the size of both vectors.

Given the equation in (14), it is possible to calculate the line loads which produce an approximation to the specified deflections $d(x_i)$ by using

$$D = CP \tag{15}$$

$$P = (C^T C)^{-1} C^T D \tag{16}$$

Since $x_i = x_j$, the C matrix is square, and equation (16) becomes

$$P = C^{-1}D \tag{17}$$

where D is an $m \times 1$ matrix specifying the surface deflections at locations x_i, C is an $m \times m$ matrix specifying the impulse surface deflection for deflection locations x_i and line load locations x_j, and P is an $m \times 1$ matrix specifying pressure values at locations x_j.

To calculate the pressure matrix P, the C and D matrices must first be specified. The actual numerical calculation of the C matrix is done by using the two vectors, x_i and x_j (which are the same), and equations (12) and (14). The length of the grating pattern is chosen to be 80 mm. Thus, both x_i and x_j are approximately of length 420, and the C matrix is about 420×420 in size. Matlab coding for the C matrix is found in Appendix C. In the coding, the number of grating periods is varied to produce overall grating lengths of approximately 80 mm. This is done because it was impossible to produce an exact 80 mm length with some gratings while keeping the grating period constant. This does not affect the calculation, since in analysis, only the middle 10 mm of the grating pattern is examined.

The calculation of the D matrix is trivial, since it only corresponds to the deflections of the grating surface and not the gaps between them. Thus, all the $d(x_i)$ values are 2.0 mm, which is the approximate depth the gratings were indented into the finger.

Once the C and D matrices are known, the pressure matrix P can be calculated from equation (17). The resulting P matrix corresponds to the pressures at locations x_j. Figure 6 shows the relationships between the deflection matrix D, pressure matrix P, and their respective locations x_i and x_j. Since the x_j vector does not include any zero values for the gaps in between, it is necessary to create a new matrix P_{new} which contains zero values interspersed in the correct locations corresponding to gaps in the grating pattern. This is also done in the matlab coding in Appendix C.

As a verification of the P_{new} vector, it is convolved with the known impulse deflection pattern $c\,(x)$, as calculated in equation (12). Figure 7 shows the resulting P_{new} corresponding to a 3.6 mm grating period, along with the resulting displacement profile D from

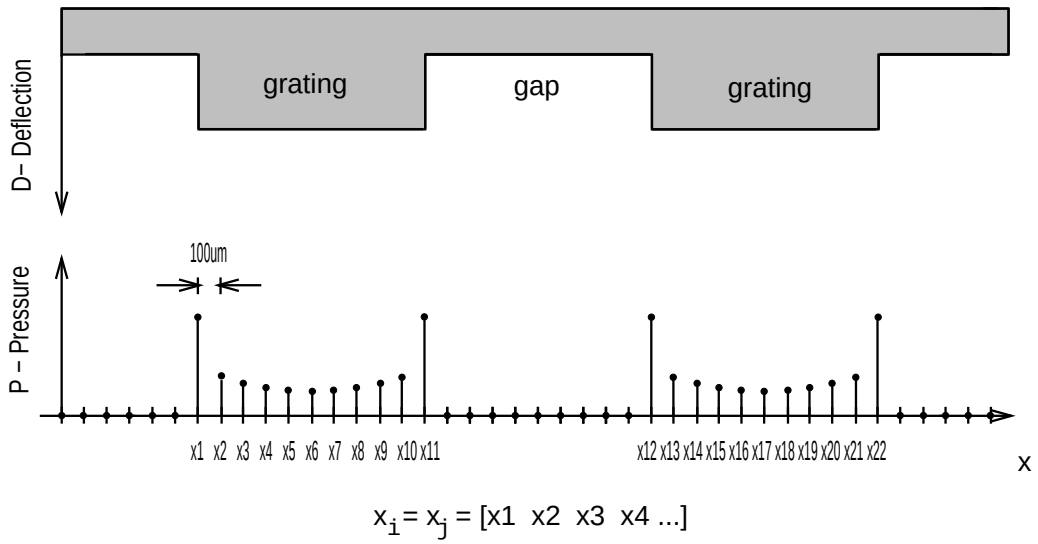

FIGURE 6. *Deflection and pressure values at locations x_i and x_j, respectively*

P_{new}. Since the deflections for the *D* matrix are 2.0 mm, this verifies that the pressure profiles within those areas are correct. Convolving this with the normal strain from equation (6) and the maximum compressive strain from equation (9) results in the normalized strain profiles shown in figure 8. These are two strain profiles which could be sensed by the mechanoreceptors underneath the skin surface.

As shown in the previous section, the maximum compressive strain is a better low-pass filter than the normal strain (see figure 4). Phillips and Johnson (1981c) found that the maximum compressive strain closely approximates the SA I mechanoreceptor response profile, while the normal strain does not. However, the responses of constructed tactile sensors in Fearing (1990) more closely matched the normal compressive strain. Because of its higher spatial frequency response, the normal strain produces a larger amplitude than the maximum compressive strain, as can be seen in figure 8. This produces a much more distinct modulation factor for the grating periods. Since it more closely approximates the tactile sensor, the normal strain is used for analysis, though comparisons with the mechanoreceptor responses using the maximum compressive strain will also be done.

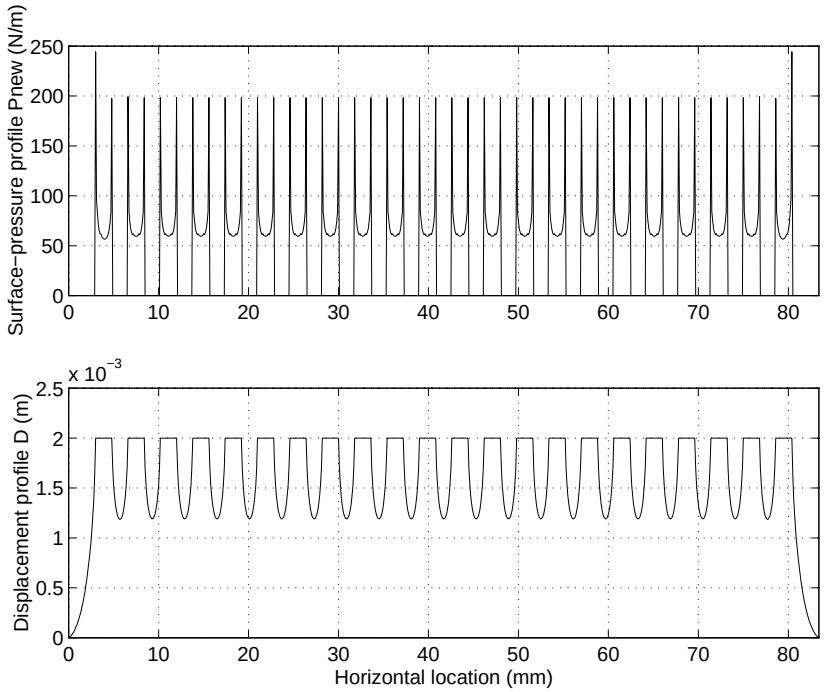

FIGURE 7. *Grating pattern with 3.6 mm grating period*

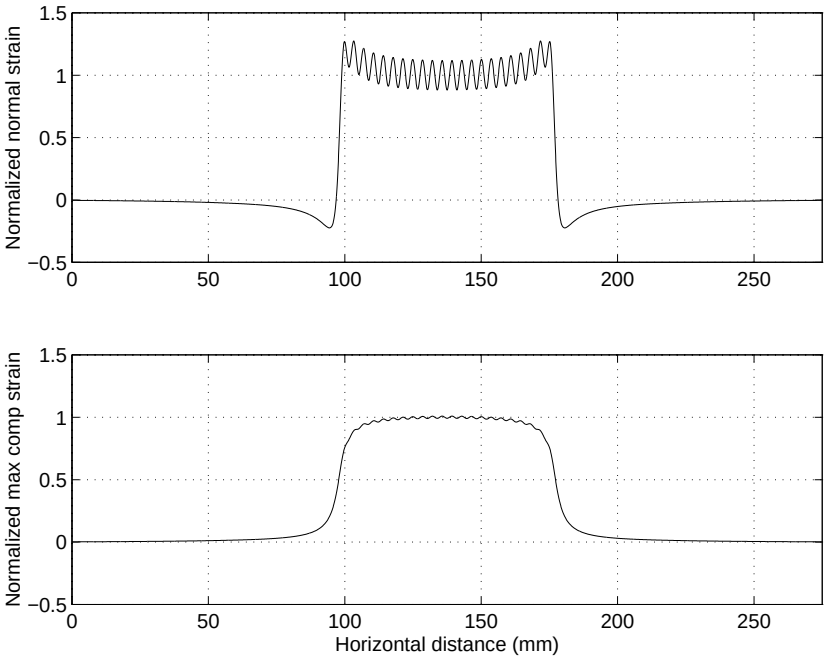

FIGURE 8. *Strain response for 3.6 mm grating period at depth = 2.7 mm*

The modulation index for the 3.6 mm grating period shown in figure 8 is 12% for the normal strain, as opposed to 0.9% for the maximum compressive strain. As can be seen, the normal strain profile is higher at the edges of the grating pattern. Because of this, the center region, which is relatively flat, is used as the estimated strain profile being presented to the finger. Unfortunately, this is not a true representation of what occurs. In reality, the grating period is long compared to the finger, and the higher strain profiles from the edges are perceived by the finger. However, due to the curvature of the fingertip, the higher edge effects are not as prevalent as they would be with a completely flat surface, since the skin surface is curving away from the deflection. This approximation is adequate for our purposes.

Figure 9 shows a plot of the modulation indices with their corresponding spatial frequencies for an SA I mechanoreceptor depth of 2.7 mm and 3.0 mm. The depths represent the range of SA I depths in the human skin with a 2.0 mm rubber layer. The figure shows the estimated bounds for the modulation indices from the strain profiles for spatial frequencies of 0.17 cycles/mm (6.0 mm grating period) up to 0.33 cycles/mm (3.0 mm grating period). As can be seen, the modulation index does not change by a large amount for the small 0.3 mm change in depth. Thus, the modulation index for a 2.7 mm depth can be used to approximate the modulation index in general.

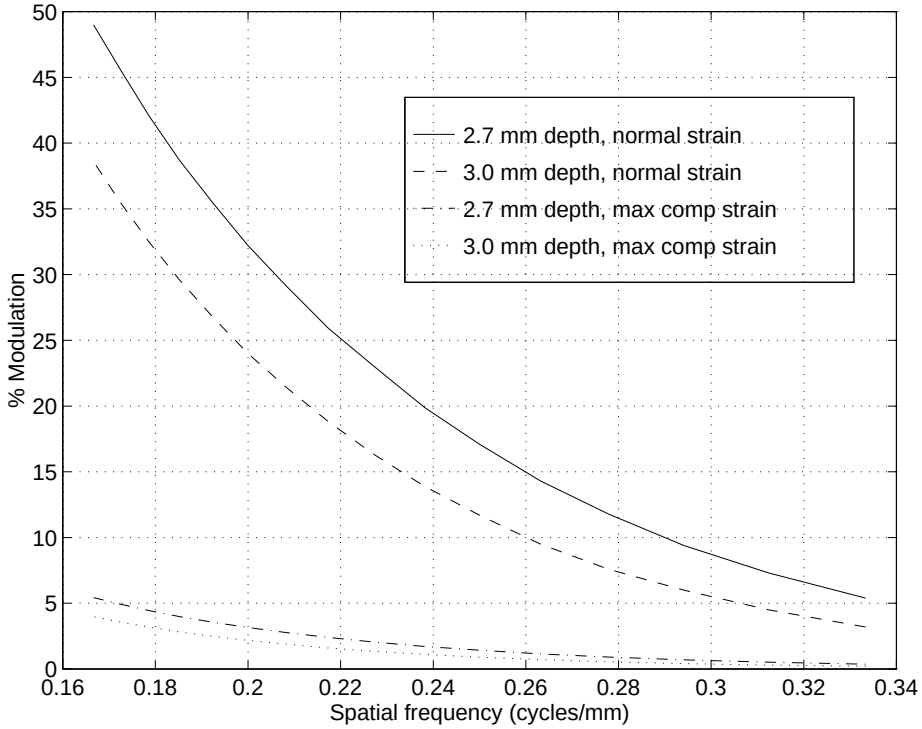

FIGURE 9. *Modelled subsurface modulation factors for square grating patterns*

3 Experimental Methods

3.1 Experimental Apparatus

In order to test a variety of different grating patterns, a system was needed which allowed for the easy interchange of test patterns, incorporated some type of force sensor, and manipulated the patterns quickly and efficiently. The force sensor was used to control the amount of force applied to the human finger, such that the application of the force was quick but not abrupt. The robot modules of the Robotworld system in the robotics lab at the University of California, Berkeley, were used as the overall controlling mechanism. The modules have 4 degrees of freedom: three translation and one rotation. The force sensor used was a Lord 15/50 Force/Torque sensor, and it was attached directly to the module. For interchangeability and easy manipulation, a circular aluminum plate was designed, which was attached to the force sensor. The plate was constructed with twelve evenly spaced rectangular slots in a circular arrangement around the perimeter. A wax block with

grating patterns milled onto its surface was inserted into each slot. The blocks fit snugly and were also held in by gravity and by the placement of the finger during testing. A detailed drawing of the apparatus is given in figure 10.

The patterns used for stimulation were created using machineable wax blocks. The surfaces of the wax blocks were smoothed down with a fly cutter, and different sized grating patterns were milled onto the surfaces using small end mill cutters. Various sized patterns were made, ranging from 2.0 mm to 20 mm periods with a 50% duty cycle. The gratings were then cut out of the wax in 25 mm x 40 mm rectangular blocks with a 30 mm x 40 mm base. Sets of gratings were made with periods that varied logarithmically and linearly. An initial group of test runs was performed to determine the general range over which all subjects could detect the existence of patterns. The final set of patterns used was composed of gratings with 3.4 mm to 5.2 mm periods, with increments of 0.2 mm. Two smooth patterns were also included in the set, and placed at opposite ends of the aluminum plate; the rest of the ten patterns were randomly placed in the remaining slots.

3.2 Experimental Procedure

Each test subject had his or her right index finger extended and kept straight by the use of a wooden splint. The splint was attached to the back of the finger and extended from the fingertip to the knuckle. The subjects then chose from an assortment of specially made 2.0 mm thick rubber fingertips, each with contours conforming to a human finger (see Appendix A for method of construction). The sole criteria for choosing a rubber fingertip was that it fit snugly over both the finger and the splint, but not so tightly as to cause discomfort. The hand was then placed on an inclined, contoured platform in a natural position, facing downwards. The right index finger was inserted through a slot in the platform and immobilized by two velcro straps, one above and one below the base of the finger. A series of grating patterns was then presented to the subject's finger, using the robot module. The robot module maneuvered the patterns beneath the finger and then raised them

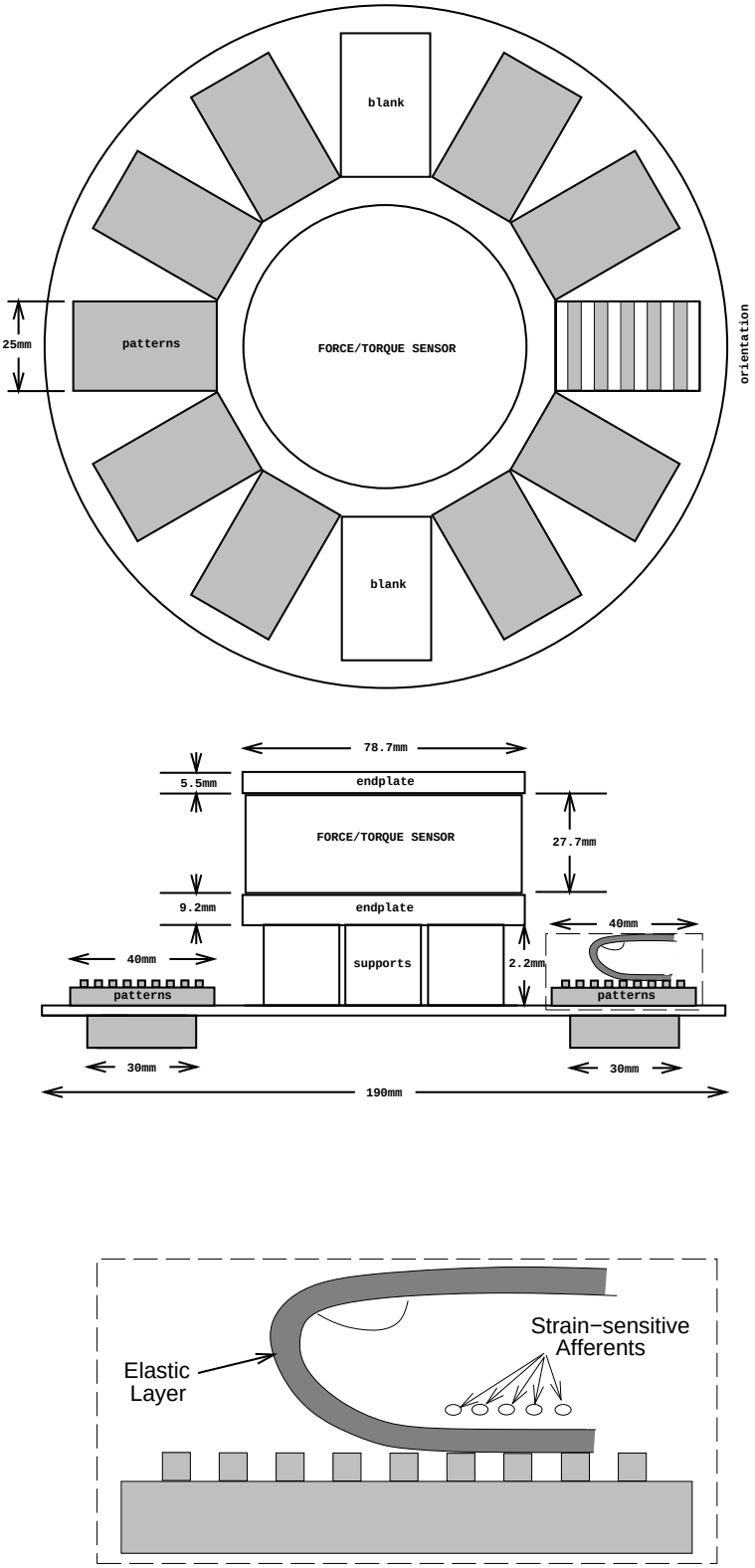

FIGURE 10. *Schematic of testing apparatus with grating and finger orientation*

into contact with the finger. Using the force sensor, the module adjusted its height until the correct contact force was applied. The grating stimulus was then presented to the finger for a span of two seconds, at which time the grating was removed from the finger. Because of robot friction, the time to reach the force setpoint varied; the general stimulus time was between 3 to 5 seconds before the pattern was removed from the finger. The overall control of the robot module is outlined in Appendix B. The entire apparatus was hidden from the view of the test subject.

The psychophysical test consisted of a group of 10 grooved patterns. Pairs of patterns were presented randomly to the subject and were either [smooth-patterned] or [patterned-smooth]. The subject then indicated which block had the pattern milled upon its surface by the use of two push-buttons. Four tests were performed, with each pattern being presented five times per test at a force of 4 N. The results were compiled over all four tests, such that every pattern was presented twenty times each. Each test took approximately twelve minutes.

3.3 Experimental Results

3.3.1 Data Analysis

Psychophysical data was derived from a total of seven test subjects, six male and one female. All subjects were volunteers associated with the robotics lab, and no criteria were used to select them. The ages of the subjects varied from 20 to 34 years of age, and the index finger sizes varied from 15 mm across the fingerpad to 20 mm across the fingerpad.

The performance of each of the seven subjects is plotted in figure 11, with percentage correct versus grating period. Choosing 75% (the midvalue between chance and perfect discrimination) as the threshold level, the threshold grating period for the test subjects varies from 3.6 mm to 5.0 mm. Here, the threshold level for each subject is considered to

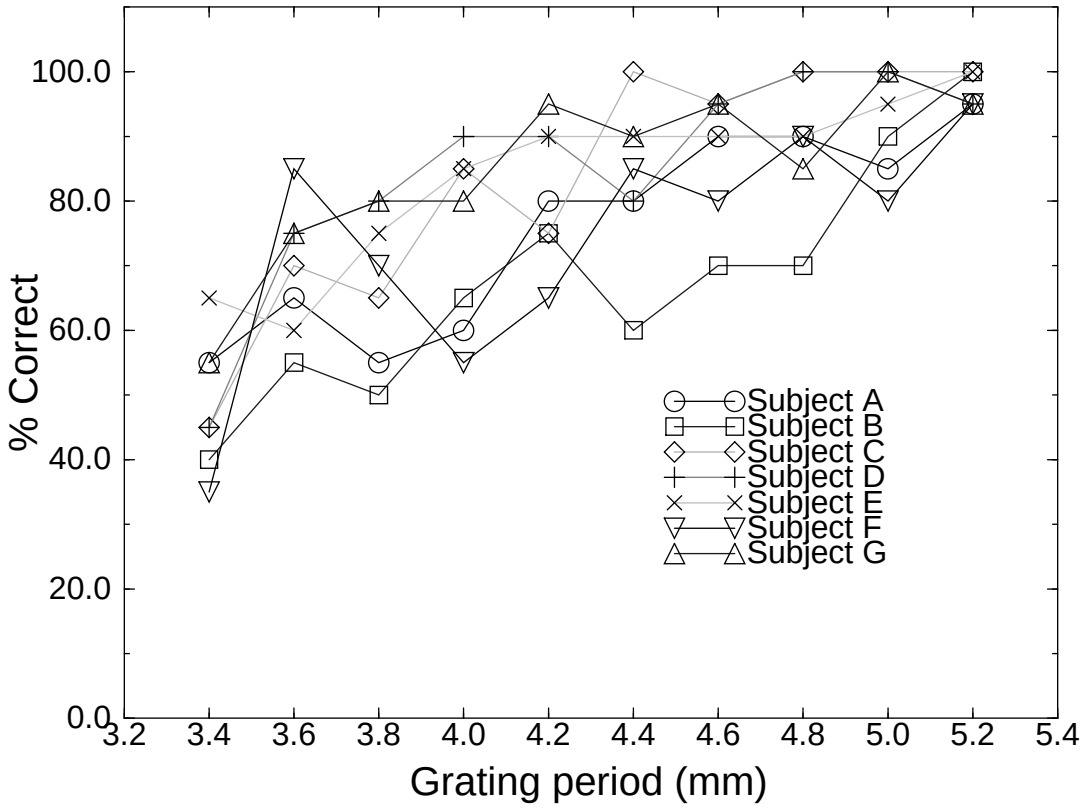

FIGURE 11. *Experimental results for each test subject*

be the grating period at which the test subject begins to accurately discern the existence of a pattern under the 2.0 mm rubber layer. The average performance of the test subjects is plotted in figure 12. Error bars show one standard deviation for each period, with the deviations varying from 2.7% correct to 12.5% correct. The average threshold grating period is 4.0 mm.

The results demonstrate that, in general, the ability to discern pattern existence increases with an increase in grating period. This makes logical sense in that as the edges of the gratings become more widely spaced apart, the pressure profile of the edges, and correspondingly the strain profile, becomes much more pronounced with respect to the DC bias. This happens because the additive effects of the line loads from two adjacent edges decreases as the distance between them increases.

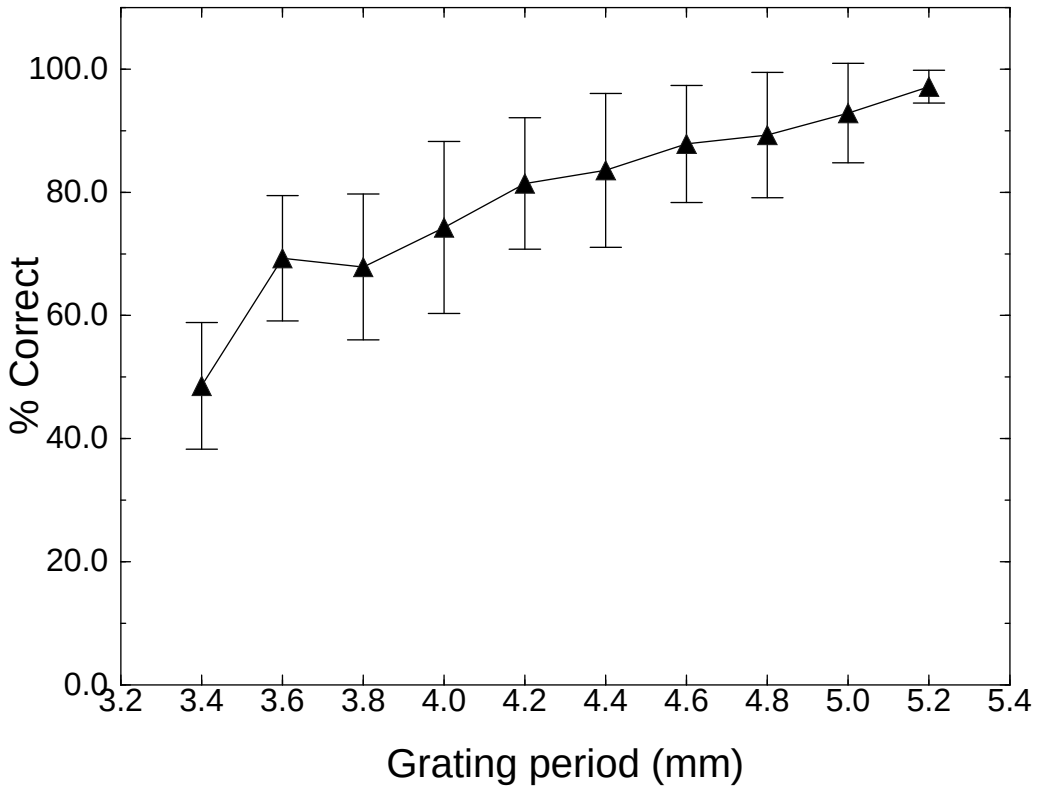

FIGURE 12. *Average percentage correct for all test subjects*

Looking at the normalized strain profile calculated from the pressure/displacement profiles, the approximate modulation factor for each of the various test subjects can be determined. The normal strain profiles for the different threshold levels of the grating periods are similar to that shown in figure 8. Thus, the normal strain profiles for the center 10 mm are enlarged and shown in figure 13 for all thresholds. For the most sensitive subject (the person with the smallest grating period threshold), the estimated modulation is approximately 12% of the DC bias. For the least sensitive subject (the person with the largest grating period threshold), the estimated modulation is approximately 24% of the DC bias. The intermediate values determined are 14%, 17%, and 20%. This suggests that for a stimulator array with high spatial detail, the largest number of bits of force resolution

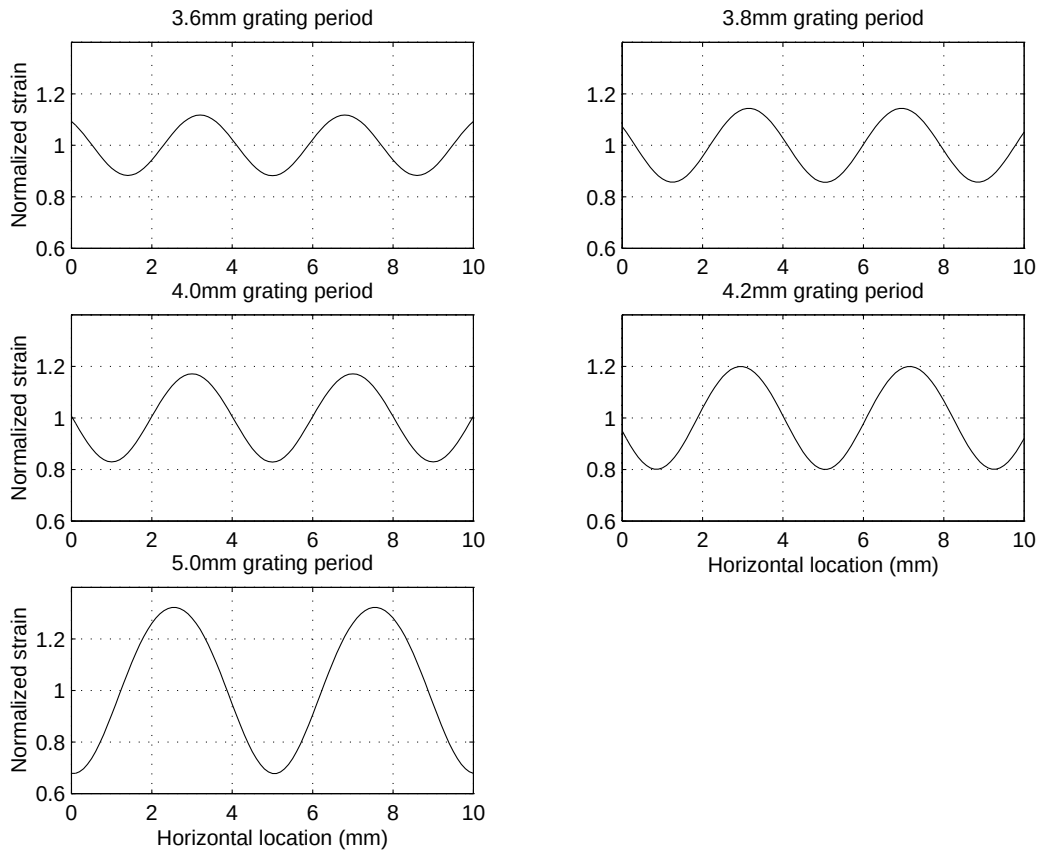

FIGURE 13. *Center 10 mm of normal strain for all threshold periods*

necessary is two or three, where two bits would give 25% ($1/2^2$) and three bits would give 12.5% ($1/2^3$). For profiles using the maximum compressive strain, the modulation factors are 0.9%, 1.1%, 1.4%, 1.7%, and 3.2%. Compared to the normal compressive strain, five to seven bits of force resolution are necessary to achieve high spatial detail.

3.3.2 Presence of Hysteresis

During all the tests, subjects reported that initial comparisons between grating patterns and smooth patterns resulted in clearer decisions than later in the test. When large grating period patterns were compared to a smooth pattern, the tactile perceptions were distinct; when smaller grating period patterns were compared to a smooth pattern, both felt smooth. However, after wearing the gloves for some time, subjects reported that patterns

became harder to discern, and that often they perceived grating patterns on both comparison surfaces, when in fact one was known to be smooth. This led to the supposition that after being under pressure from the rubber fingertip for several minutes, the finger started to partially retain the deformations from previous grating patterns instead of quickly recovering from them as it did at the beginning of the test. This resulted in the perception of a pattern when the fingertip was placed against a smooth surface, which caused confusion when compared to another detectable pattern. In an attempt to quantify the hysteresis effect which was present, an analysis of the experimental data was done.

All responses were examined, and data was compiled on sequences of patterns presented to the test subjects. One analysis looked at all sequences which produced incorrect responses. The sequences were broken down into four groups: {smooth-[smooth-pattern]} (SSP), {pattern-[smooth-pattern]} (PSP), {smooth-[pattern-smooth]} (SPS), and {pattern-[pattern-smooth]} (PPS), where the square brackets denote the testing of a pattern/smooth pair. The data from these sequences is shown in table 1.

TABLE 1. Sequence analysis of all incorrect responses

Subject	SSP	PSP	SPS	PPS	Total
A	18	18	4	10	50
B	16	26	12	13	67
C	10	8	6	7	31
D	8	5	9	7	29
E	8	10	10	3	31
F	16	18	11	10	55
G	6	11	9	3	29

As can be seen, no particular sequence can be said to dominate any other sequence, although one subject had a definitive sequence of errors (subject B, sequence PSP) which was greater than the rest. The lack of conclusive results could be explained by the small number of errors most subjects exhibited. For a better quantitative analysis of hysteresis, more tests need to be performed in order to get a larger number of errors for comparison.

Another analysis looked at all the data gathered from the experiment. In this case, the ten grating patterns were split into three groups: the fine patterns (3.4 mm to 4.0 mm grating periods), the middle patterns (4.2 mm and 4.4 mm grating periods), and the coarse patterns (4.6 mm to 5.2 mm grating periods). Data was then compiled on the sequences {coarse-[smooth-coarse/coarse-smooth]} (CC) and {coarse-[smooth-fine/fine-smooth]} (CF). This is shown in table 2.

TABLE 2. Comparison of CC and CF sequences

Subject	# CC correct/ incorrect	# CF correct/ incorrect	% CC correct	% CF correct
A	18/3	14/6	86	70
B	11/3	11/8	79	58
C	20/0	12/4	100	75
D	22/0	12/2	100	86
E	11/0	16/4	100	80
F	15/1	11/3	94	79
G	18/1	14/3	95	82

As can be seen, every test subject shows a greater correct percentage of CC sequences than of CF sequences. The difference between the two sequences varies from 13% up to 25%, with the average difference being 17%. This could possibly be attributed to hysteresis, although another reason for this difference is that the finer patterns corresponded to levels which were below the threshold period of some of the subjects. Still, it is possible that part of the difference is a result of the hysteresis effect, which would be present more during a (CF) sequence than during a (CC) sequence. This would happen because the hysteresis effects would be more easily confused with the finer patterns, which have smaller modulation factors, than with the coarser patterns, which have larger modulation factors.

In order to quantify the hysteresis effects to a better degree, it is necessary to perform other experiments. One such experiment would be to present a large number of smooth patterns with a small number of grating patterns randomly interspersed with them.

The subjects would then be asked if they could detect a pattern on the blocks presented. In general, hysteresis would cause the subject to perceive patterns after a large grating pattern had been presented. This would help determine which sizes of grating periods would be more likely to produce hysteresis effects. This and other experiments are left as future work to be performed.

3.3.3 Comparison with other Tests

In a comparison with Phillips and Johnson's (1981a) grating resolution test, in which they tested the human ability to distinguish the orientation of two orthogonal gratings, the approximate grating period at which they achieved 75% correct judgement was at 2.0 mm, as compared to the 4.0 mm grating period average threshold for this experiment. Although the result from this test is double that of Phillips and Johnson, their orientation test was done directly against the surface of the fingertip while this test was done with a 2.0 mm rubber layer. Since a large amount of information is filtered out by the rubber layer, it is necessary for the threshold grating period to be wider than the period necessary for direct skin contact. Therefore, the results of the two experiments are consistent.

3.4 Lack of Fit and Inconsistencies

Along with the model and experimental data detailed in this paper, it is necessary to list and quantify the possible sources of errors, inconsistencies, and variable factors which could influence the results discovered. To begin with, there are errors in the testing apparatus itself and problems with the testing procedures which can not be controlled. The hysteresis effects discovered must also be considered, along with inconsistencies of the half-plane elastic model. Finally, there are several extraneous factors which could have influenced the results derived here, such as the sensitivity of the human finger to slipping and thermal conductivity. These factors are addressed in the following sections.

3.4.1 Apparatus and Testing Errors

While acquiring experimental data from test subjects, several inherent problems associated with the testing apparatus arose. The Lord sensor, with no forces or loads placed upon it, had measurement errors of up to +/- 0.2 N of force. Because of this variance, it was sometimes possible to achieve a limit cycle when trying to reach the desired application force. The module would oscillate around the setpoint, just outside of the threshold level established (see Appendix B), and this would sometimes allow the subject to glean more information from the grating pattern being presented.

Another problem experienced was with the z-axis control of the robot module. Although the stepper motor in the z-axis was extremely precise, the axis sometimes got stuck while moving up to a position associated with the specified force. While the program thought that the module was moving in the z-axis, it would actually be stationary. The force value read in would remain constant, and the program would continue to try to move the module to higher setpoints until it reached a point at which the force applied to the z-axis overcame the friction. Then, the module would suddenly jump up to the current z-axis position at a much higher force than desired. The increased force from the abrupt movement would often give the subject more information than would be received from the normal force measurement.

One other problem with the testing apparatus was that the splint/velcro strap arrangement did not completely immobilize the finger, since it did not physically restrain every degree of freedom of the finger. If the subjects so desired, they could move their finger from side-to-side or forwards-backwards, although at the outset, they were requested to keep their finger totally relaxed and immobile. Although it was physically possible to adhere the subjects' finger/hand to a surface for complete immobility, this was rejected because it would be uncomfortable and impractical.

Another portion of error was due to the fact that the overall test of 20 trials per pattern was broken down into four shorter tests of 5 trials per pattern. This was done in order

to allow the subjects time to rest their finger and to make the testing times, which were on the order of twelve minutes, bearable. However, this resulted in the problem of trying to position the finger in the same location during each test. Although efforts were made to do this, variance could have occurred because of slightly different finger surface areas being in contact with the grating patterns. What complicated matters even more was that all four tests were not given in one sitting. In general, most subjects could only endure the monotony of two tests at any one time, and often the four tests would be split over several days, due to both the availability of the subjects and the tester. Thus, other factors like daily temperament or alertness could have affected the outcome of the tests.

3.4.2 Effects of Hysteresis

As was discussed in section 3.3.2, hysteresis effects are a factor when wearing a rubber fingertip for long periods of time. Although no quantitative conclusions can be drawn from the experimental data, hysteresis was subjectively perceived by all test subjects. This is believed to be caused by the retention of surface deformations from large grating patterns. When these deformations are placed against a smoother pattern, the resulting strain profile may have a large enough modulation factor to confuse the SA I mechanoreceptors into believing a pattern is being presented. This amplitude then becomes confused with the amplitude from the modulation factor of the finer patterns, resulting in errors in perception. Thus, the hysteresis decreases the amplitude resolution capabilities of the finger and induces errors in judgment. Future experiments will be performed to quantify the effects of hysteresis.

3.4.3 Model Inconsistencies

One possible source of inconsistency is a result of the inadequacies of the model used. In the model, it is assumed that the rubber fingertip and skin form one continuous layer with a modulus of elasticity of $4x10^5$ N/m^2. However, this is not a valid assumption, as the skin's modulus of elasticity, which is measured as approximately $5x10^4$ N/m^2, is

much lower than the rubber's. This produces a discontinuity between the two surfaces, which is not taken into account by the model. Although finite element analysis could have been used to calculate the effects of the discontinuity and possibly provide a better result, the fact that there does not exist an accurate model of the actual tissue structure beneath the skin would have rendered the finite element analysis useless. The exact effects of the bone structure against which the tissue is compressed is also unknown, and provides more uncertainty. Thus, although the half-plane elastic model is a reasonable first order assumption and corresponds to the same physiological measurements as seen in Phillips and Johnson (1981c), it may not be completely applicable in this case.

3.4.4 Sensitivity to Slipping

Since the fingertip is not completely flat, contact between the fingertip and the grating pattern may have produced small amounts of slipping when the grating was pushed vertically into the fingertip by the robot module. This could have improved a subject's ability to distinguish the patterns, since more information is available to the mechanoreceptors in the skin. However, in this case, slippage is not perceived by the SA I mechanoreceptors, since they are mainly sensitive only to skin surface deformations. Instead, two other types of nerve endings, the Meissner corpuscles (FA or FA I mechanoreceptors), and the Pacinian corpuscles (PC or FA II mechanoreceptors) are stimulated. As found in Srinivasan et al. (1990), the FA I units are extremely sensitive to slippage when small features are moved across the surface of the skin, such as those perceived from the grating patterns. The FA II units, on the other hand, are extremely sensitive to high frequency vibrations. These vibrations could have been evoked from the sliding of the fingertip over the grating patterns (Johansson and Westling 1987). Thus, data besides the surface deformations could have been used to determine if a pattern was present beneath the rubber layer.

3.4.5 Thermal Conductivity

Another factor which may have affected the ability of the subjects to distinguish grating patterns is the thermal conductivity of the wax patterns. Given that the patterns had a 50% duty cycle, they had twice the overall thermal resistance of smooth gratings. Therefore, it is possible for people to determine the existence of patterns from the different temperature gradients induced by the different thermal conductivities. However, this effect is reduced significantly since the rubber fingertip worn by the subjects has a low thermal conductivity (3.77×10^{-4} Cal-cm/sec-cm^2/°C).

4 Discussion

The tests performed show that most people can feel grating patterns with periods of approximately 4.0 mm with a 2.0 mm rubber layer. Given the strain model, the detectable modulation index (amplitude over DC bias) varies from 12-24% for the subjects tested. These results show that the sensations from a 2.0 mm tactile array with three bits of information and a 2.0 mm rubber layer should be indistinguishable from the sensations produced by wearing a 2.0 mm thick glove and touching the actual contour or shape. Thus, the sensations perceived by the fingertip in figure 1 and figure10 are equivalent given these parameters. Furthermore, hysteresis is an important factor in perception and must be taken into account when designing and using tactile stimulators with silicone rubber layers, especially with rapidly changing contacts.

This work was funded by NSF-PYI Grant IRI-9157051.

Appendix A

Construction of 2.0 mm layer fingertips

In order to construct rubber fingertips with an accurate 2.0 mm thickness, several methods were considered. Looking at common gloves which were available, all either had thicknesses much less than the 2.0 mm needed or were made of an unsuitable material. Initial attempts to create 2.0 mm thick gloves by putting multiple layers of known sizes over each other were unsuccessful, mainly because of slip in between the multiple layers, the extreme difficulty in putting all the layers on, and the discomfort resulting from the very tight fit. Also, while experimenting with normal latex gloves, it was noted that although the fingertips were constructed uniformly and cylindrical for general use, there were air gaps in areas, especially around the joints and at the tip. This caused an uneven pressure distribution around the entire finger and resulted in a fit which was not completely snug. Thus, it was decided that rubber fingertips made from molds of the test subjects' fingers would be used, and that the fingertips would be made from a single mold to eliminate multiple layers. This would result in a single layer, contoured fingertip which would fit snugly on the finger and would provide an even pressure distribution around the entire finger. The method to produce such a mold was as follows.

First, several layers of thin latex gloving were placed over a person's index finger, and a plaster mold of the finger was constructed using Plaster of Paris. Once this mold had hardened sufficiently, the finger was removed and several notches were cut into the perimeter surrounding the top of the impression. After the entire mold had finished hardening, a wax impression of the finger was created, which included the notches. Using this wax impression as an inner mold, a 2.0 mm thick layer of gloving was placed over it up to, but not including, the notches. The 2.0 mm layer was constructed by placing several layers of latex glove fingertips of known thickness over each other. Then, another plaster mold of this new finger was made, with the notches impressed into the plaster. Once the mold had hardened sufficiently, the wax finger was taken out and the latex layers were removed.

Using the wax mold as the inner mold and the plaster mold as the outer one, Dow Corning HSII silicone rubber was poured into the outer plaster mold. The inner wax mold was then inserted into the outer mold such that the notches coincided with each other and were clamped down securely. This insured a uniform 2.0 mm layer all around the inner mold. Once the rubber hardened, the outer plaster mold was broken away and the rubber mold was removed, producing a 2.0 mm layer rubber fingertip, custom made for each subject.

Appendix B

Control program

The control program for the module and plate was a C++ program using library functions utilizing the real-time kernel commands available on Robotworld. Inputs from the Lord sensor and from the subject were accessed using these functions, and the program adjusted the circular aluminum plate and patterns accordingly. Once the entire assembly was attached to the robot module, the Lord sensor readings were initialized to zero, and the aluminum plate was moved to its start configuration. After the test subject's finger was in place, an initialization run was performed to determine an appropriate start height so that patterns could be moved quickly into contact with the finger. Once this had been determined, one of the smooth patterns was presented to the subject's finger for calibration. Once the subject had felt the pattern for a sufficient amount of time, the test began. The module removed the smooth pattern and rotated a test pattern underneath the finger. It was raised to the initialized height and then slowly moved upwards while reading the z-axis force value from the force sensor. The program used a simple control feedback loop to move along the z-axis. If the force reading was far away, the increments were large; once the force reading was within a threshold range, smaller increments were used. The desired force was considered to have been reached when the sensor reading was within +/- 50 mN of the desired force. After the desired force had been achieved, the pattern was held under the finger for a span of two seconds and then removed. The module would then rotate to two intermediate values before moving to the second pattern to be presented. This was done to confuse the test subjects in case they were attempting to listen to the rotations of the module to help in determining what patterns were presented. Two smooth patterns were used instead of one to also confuse the subject. Once the second pattern was presented and removed, the subject was allowed time to indicate which of the two patterns they believed to contain a grating pattern. Upon receiving a response, the module once again rotated to two intermediate values before presenting the next pair of patterns. This

was continued until all patterns had been tested five times each. The sequence of patterns presented and the method of presentation ([smooth-patterned] or [patterned-smooth]) was randomly computed and different for each separate trial.

Appendix C

Matlab coding for calculation of the C, P, and D matrices

The matlab coding used in the various calculations is listed here. The function "profile" creates and computes the matrices *P, C, D,* and P_{new} discussed in section 2.2. The function "deflect" creates the impulse deflection vector from equation (12), which is used to calculate the strain profiles. The function "strain" calculates the two different types of strains, the normal strain and the maximum compressive strain.

REFERENCES

Cohn, M. B., Lam, M., and Fearing, R. S. 1992. Tactile feedback for teleoperation. *Telemanip. Tech. - SPIE Proc.* 1833, Nov. 15-16.

Fearing, R. S. 1990. Tactile sensing mechanisms. *Int. J. Robot. Res.* 9(3):3-23.

Fearing, R. S., and Hollerbach, J. M. 1985. Basic solid mechanics for tactile sensing. *Int. J. Robot. Res.* 4(3):40-54.

Goldstein, E. B. 1980. *Sensation and Perception.* Belmont, CA: Wadsworth Pub. Co.

Hasser, C. J., and Weisenberger, J. M. 1993. Preliminary evaluation of a shape-memory alloy tactile feedback display. *Adv. Rob. Mechatr. Hapt. Interf. ASME.* 49:73-80.

Johansson, R. S., and Westling, G. 1987. Signals in tactile afferents from the fingers eliciting adaptive motor responses during precision grip. *Exp. Brain Res.* 66:141-154.

Kontarinis, D. A., and Howe, R. D. 1993. Tactile display of contact shape in dextrous telemanipulation. *Symp. Hapt. Interf. Virt. Env. Teleop. Sys. ASME Wint. Ann. Mtg.* Nov. 28-Dec. 3.

LaMotte, R. H., and Srinivasan, M. A. 1987. Tactile discrimination of shape: Responses of slowly adapting mechanoreceptive afferents to a step stroked across the monkey fingerpad. *J. Neurosc.* 7(6):1655-1671.

Phillips, J. R., Johansson, R. S., and Johnson, K. O. 1992. Responses of human mechanoreceptive afferents to embossed dot arrays scanned across fingerpad skin. *J. Neurosc.* 12(3):827-839.

Phillips, J. R., and Johnson, K. O. 1981a. Tactile spatial resolution. I. Two-point discrimination, gap detection, grating resolution, and letter recognition. *J. Neurophysiol.* 46(6): 1177-1191.

Phillips, J. R., and Johnson, K. O. 1981b. Tactile spatial resolution. II. Neural representation of bars, edges, and gratings in monkey primary afferents. *J. Neurophysiol.* 46(6):1192-1203.

Phillips, J. R., and Johnson, K. O. 1981c. Tactile spatial resolution. III. A continuum mechanics model of skin predicting mechanoreceptor response to bars, edges, and gratings. *J. Neurophysiol.* 46(6):1204-1225.

Srinivasan, M. A., Whitehouse, J. M., and LaMotte, R. H. 1990. Tactile detection of slip: Surface microgeometry and peripheral neural codes. *J. Neurophysiol.* 63(6):1323-1332.

Timoshenko, S. P., and Goodier, J. N. 1970. *Theory of elasticity, 3rd ed.* New York: McGraw-Hill.

Vallbo, A. B., and Johansson, R. S. 1979. Tactile sensibility in the human hand: Relative and absolute densities of four types of mechanoreceptive units in glabrous skin. *J. Physiol. (London)*. 286:283-300.